Program Digest, 2019 IEEE International Ultrasonics Symposium (IUS)
Glasgow, Scotland, October 6-9, 2019

Design of dual-frequency piezoelectric micromachined ultrasonic transducers

Lixiang Wu
School of Electronics and Information
Hangzhou Dianzi University
Hangzhou, China
wulx@hdu.edu.cn

Xuyuan Chen
Department of Microsystems
University of Southeast Norway
Borre, Norway
Xuyuan.Chen@usn.no

Gaofeng Wang
School of Electronics and Information
Hangzhou Dianzi University
Hangzhou, China
gaofeng@hdu.edu.cn

Qifa Zhou
Department of Biomedical Engineering and Ophthalmology
University of Southern California
Los Angeles, USA
qifazhou@usc.edu

***Abstract*—A piezoelectric micromachined ultrasonic transducer (pMUT) operating at dual-frequencies (3.75 MHz and 18 MHz) was designed to achieve an ultrasound-on-a-chip solution for next-generation biomedical applications. Unlike transducers using two or more single-frequency ultrasonic resonators to generate dual-frequency ultrasound, every element of dual-frequency pMUTs exhibits dual-resonant response simultaneously. Electrode configurations for the dual-frequency pMUT were optimized using finite element analysis (FEA). Simulations for dual-actuations with both inner and outer ring electrodes showed that the two resonant modes are superimposed without significant vibrational crosstalk, and result in high-quality dual-frequency acoustic radiation in water.**

***Index Terms*—piezoelectric micromachined ultrasonic transducer, dual frequency, ring electrode, ultrasound-on-a-chip, finite element analysis**

I. Introduction

Dual-frequency ultrasonic transducers for advanced biomedical applications were developed three decades ago, which were based on multiple piezoelectric layers or blocks. [1]–[3] And the development of dual-frequency ultrasonic transducers has been studied for a long time. However, most dual-frequency ultrasonic transducers are still fabricated by dividing and/or assembling bulk piezoelectric materials, which adds additional complexity to fabrication and potential degradation in beamforming performance. [4]

In contrast to bulk ultrasonic transducers, ultrasonic transducers based on microelectromechanical systems (MEMS) technology are better for mass fabrication, which consists of pMUTs and capacitive micromachined ultrasonic transducers (cMUTs). The previous studies indicate that a pMUT can exibit dual-frequency resonances on its vibrating membrane. [5], [6] Also, it has been reported that the bandwidth of pMUTs can be broadened by merging multiple resonances on a rectangular diaphragm immersed in water. [7]–[9]

To date, dual-frequency pMUTs based on a single vibrating membrane have not been reported. An important challenge to the realization of a dual-frequency pMUT device with a single membrane is elimination of vibrational crosstalk between the two resonant modes of the diaphragm. To overcome this challenge, we propose a dual-frequency pMUT design based on a single diaphragm utilizing two ring electrodes.

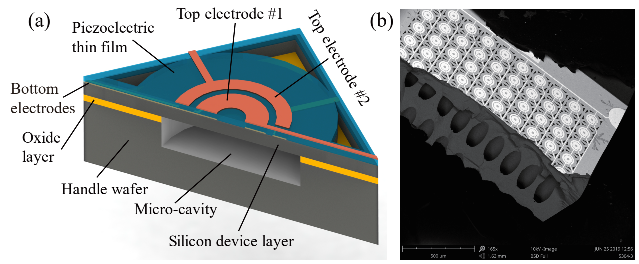

Fig. 1. (a) illustrates a unit cell of dual-frequency pMUTs and (b) presents the dual-frequency pMUT array fabricated in the first round experiment.

II. Conceptional design

Dual/Multi-eletrode pMUTs have been studied in previous work for particular purposes such as increasing transmit sensitivity, [10], [11] spliting the transmiter and receiver, [12] utilizing more resonant frequencies. [13] However, these dual/multi-eletrode pMUTs only operate at alternate resonant frequencies sequentially but not simultaneously. Inspired by the design of dual-eletrode pMUTs, we designed a dual-frequency pMUT with two ring electrodes, which aimed to excite the first two resonances simultaneously. As shown in Figure 1a, the dual-frequency pMUT has two ring electrodes instead of a disk electrode and/or a single ring electrode that are usually used in traditional pMUTs. Figure 1b shows a 10 by 10 array of dual-frequency pMUTs, which were fabricated in the first round experiment using a standard pMUT process flow. [14] The applied dual ring electrodes are straight-forward to implement in the standard pMUT process flow by changing a single metal mask and therefore do not significantly increase the cost and complexity of the fabricated devices.

III. Modeling and Optimization

A. Operating frequencies

The traditional pMUT with a single disk electrode operates at the first resonant frequency of its diaphragm. In contrast, the dual-frequency pMUT device using two ring electrodes on a single piezoelectric film diaphragm is designed to operate at the first two resonant frequencies. The first two natural frequencies can be expressed as

$$f_{1,2} = \frac{\lambda_{1,2}^2}{2\pi r^2}\sqrt{\frac{D}{\rho h}}, \tag{1}$$

where the dimensionless frequency parameters λ_1^2 and λ_2^2 equal to 10.216 and 39.771; r, h, D, and ρ are the radius, thickness, flexural rigidity, and mass density of the diaphragm. [15] The λ_2^2-to-λ_1^2 ratio is about 3.9. When the pMUT is submerged in water and its vibrating diaphragm has one side in contact with water, the ratio of the two resonant frequencies, $f_{1,2}^{'}$, is modified and becomes

$$f_{1,2}^{'} = \frac{f_{1,2}}{\sqrt{1+\beta_{1,2}\frac{\rho_w}{\rho}\frac{r}{h}}}, \tag{2}$$

where the non-dimensionalized added virtual mass incremental factors β_1 and β_2 equal to 0.46674 and 0.27231 respectively and ρ_w represents the mass density of water. [16] The design of the dual-frequency pMUT begins with the selection of operating frequencies, of which the higher frequency is specified as 18 MHz for sensing higher order harmonic vibrations. According to (1) and (2), the lower operating frequency is estimated to be 3.75 MHz, which is exactly in the range of microbubble resonance (about 1–6 MHz). The two operating frequencies are favorable for dual-frequency contrast imaging. [4]

B. Optimization of electrode configurations

To simplify the design process, we analyze the dual-electrode structure, optimize device parameters, and verify the prototyping model by finite element analysis (FEA) using COMSOL Multiphysics 5.3a. Figure 2 shows the geometry and materials of the FEA model of a single-electrode pMUT. The default voltages of the two bottom electrodes were set to zero and the voltage amplitude of both top electrodes was set to 12 V. Multiple positions and widths of the top electrode after geometric discretization were swept. The average displacements of the diaphragm topside for each of the swept data point cases were calculated and mapped as shown in Figure 3a, where two peaks at 3.75 MHz and 18 MHz were found under all swept conditions. In addition, as shown in Figure 3b, the average displacement profiles at the two peak frequencies were extracted and the displacement ratios for the cases of 3.75/18 MHz and 18/3.75 MHz were calculated. Peaks at the two profiles of displacement ratios indicate that the displacements at 3.75 MHz and 18 MHz were extremely unbalanced.

By optimizing the position and dimension of each ring electrode on which the excitation signal is applied, we found that the peak deflection amplitude of the diaphragm occurs

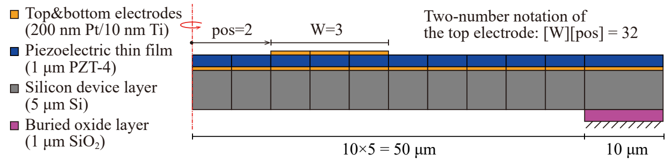

Fig. 2. The two-dimensional model for finite element simulations.

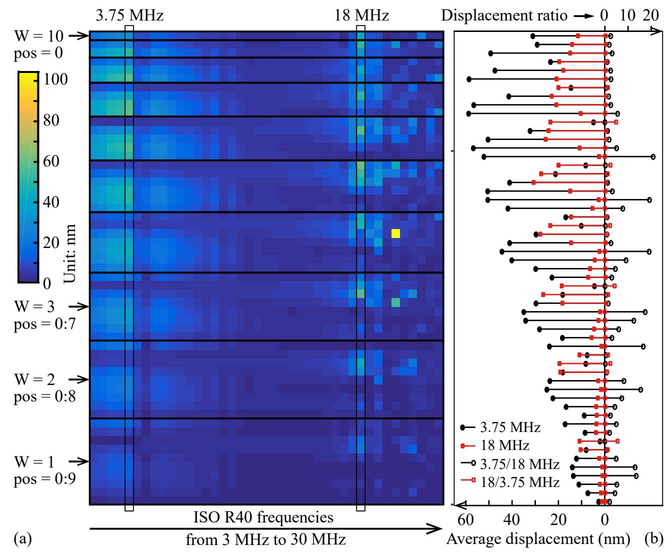

Fig. 3. The variation of average displacement with the position and width of a single ring electrode (a); the average displacement curves for the first two resonant frequencies and the displacement ratio of them (b).

at the first resonant frequency but appears minimum at the second resonant frequency. Similarly, for the alternate case, the opposite relationship was observed. Based on this physical phenomenon, two concentric ring electrodes, *e.g.*, one inner ring electrode and one outer ring electrode were designed on the diaphragm. The inner ring electrode was used for exciting the first resonance at 3.75 MHz, and the outer ring electrode was used for exciting the second resonance at 18 MHz.

In addition, the intersection between the two ring electrodes should be avoided. Figure 4 presents the candidate configurations for the inner ring electrode (in green) and the outer ring electrode (in yellow). The optimal combination was found to be W=3, pos=2 and W=2, pos=6, which is shown in Figure 4.

IV. Multiphysics Simulation

A transient analysis was conducted to evaluate the transmit-mode impulse response of the dual-frequency pMUT. The input pulses (pulses #1 and #2) are two sinusoidal waves with center frequencies at 3.75 MHz and 18 MHz and amplitudes of 12 V and 24 V, respectively. The pulses were each apodized by convolution with an identical Blackman window.

Figure 5a and b show the frequency response in terms of displacement and pressure for pulse #1 and pulse #2 applied individually to respective electrodes, as well as both pulses applied simultaneously, where the pulses #1 and #2 were

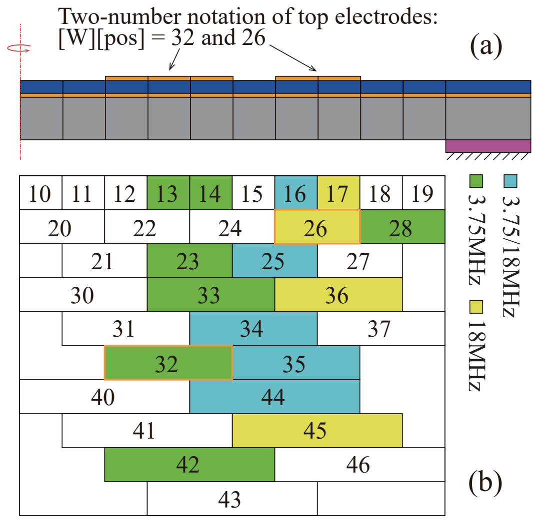

Fig. 4. (a) shows the optimal dual-top-electrode model; (b) presents the feasible combinations of two top electrodes.

applied to the top ring electrodes 32 and 26, respectively. Displacement of the diaphragm was measured at its center and acoustic pressure was measured at a distance of 0.62 mm along the acoustic axis. For a single pMUT element, there were two operating frequency bands in the frequency domain: the first frequency band was centered around 3.75 MHz with -6 dB fractional bandwidth of 46.9%, while the second frequency band was centered around 18 MHz with -6 dB fractional bandwidth of 11.4%. As is illustrated in Figure 5, the simulated response of the device to a driving signal composed of a combination of pulse #1 and pulse #2 was almost identical to the combination of the individual output responses of the system to separate inputs of pulse #1 and #2. This superposition effect holds for both the simulated displacement and the acoustic pressure, which indicates that the first two resonant modes occur together and are superimposed on the diaphragm of the dual-frequency pMUT.

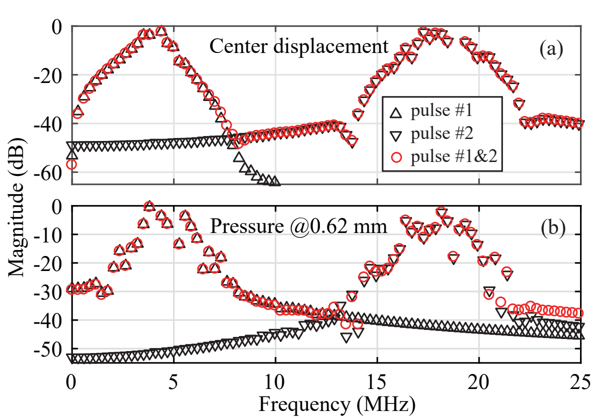

Fig. 5. (a) and (b) present the responses of center displacement and acoustic pressure in the frequency domain under different actuations.

V. Conclusion

In conclusion, a comparison of the impulse response of the dual-frequency pMUT with that of two individual single-frequency pMUTs operating at the same frequencies, suggests that the dual-frequency pMUT is equivalent to two single-frequency pMUTs in basic acoustic performance. For fine pitched arrays, such as high frequency devices, where available device area is at a premium, dual-frequency pMUTs have significant advantages over a combination of two single-frequency pMUTs in terms of device dimensions, transmit sensitivity, power consumption, and production cost. Therefore, the dual-frequency pMUT holds great promise for ultrasound-on-a-chip technology.

References

[1] S. De Fraguier, J.-F. Gelly, L. Wolnerman, and O. Lannuzel, "A novel acoustic design for dual frequency transducers resulting in separate bandpass for color flow mapping (cfm)," in *IEEE Symposium on Ultrasonics*. IEEE, 1990, pp. 799–803.

[2] J. A. Hossack and B. A. Auld, "Improving the characteristics of a transducer using multiple piezoelectric layers," *IEEE transactions on ultrasonics, ferroelectrics, and frequency control*, vol. 40, no. 2, pp. 131–139, 1993.

[3] S. Saitoh, M. Izumi, and Y. Mine, "A dual frequency ultrasonic probe for medical applications," *IEEE Transactions on Ultrasonics, Ferroelectrics, and Frequency Control*, vol. 42, no. 2, pp. 294–300, 1995.

[4] K. Martin, B. Lindsey, J. Ma, M. Lee, S. Li, F. Foster, X. Jiang, and P. Dayton, "Dual-frequency piezoelectric transducers for contrast enhanced ultrasound imaging," *Sensors*, vol. 14, no. 11, pp. 20 825–20 842, 2014.

[5] C. Chao, T.-Y. Lam, K.-W. Kwok, and H. L.-w. Chan, "Piezoelectric micromachined ultrasonic transducers with rectangular diaphragms for dual-frequency applications," in *Micro (MEMS) and Nanotechnologies for Defense and Security*, vol. 6556. SPIE, 2007, p. 65561J.

[6] A. Hajati, D. Latev, D. Gardner, A. Hajati, D. Imai, M. Torrey, and M. Schoeppler, "Three-dimensional micro electromechanical system piezoelectric ultrasound transducer," *Applied Physics Letters*, vol. 101, no. 25, p. 253101, 2012.

[7] Y. Lu, O. Rozen, H.-Y. Tang, G. L. Smith, S. Fung, B. E. Boser, R. G. Polcawich, and D. A. Horsley, "Broadband piezoelectric micromachined ultrasonic transducers based on dual resonance modes," in *IEEE 28th International Conference on Micro Electro Mechanical Systems (MEMS)*. IEEE, 2015, pp. 146–149.

[8] T. Wang, T. Kobayashi, and C. Lee, "Micromachined piezoelectric ultrasonic transducer with ultra-wide frequency bandwidth," *Applied Physics Letters*, vol. 106, no. 1, p. 013501, 2015.

[9] C. Sun, Q. Shi, M. S. Yazici, T. Kobayashi, Y. Liu, and C. Lee, "Investigation of broadband characteristics of multi-frequency piezoelectric micromachined ultrasonic transducer (mf-pmut)," *IEEE Sensors Journal*, vol. 19, no. 3, pp. 860–867, 2019.

[10] F. Sammoura, S. Akhari, N. Aqab, M. Mahmoud, and L. Lin, "Multiple electrode piezoelectric micromachined ultrasonic transducers," in *IEEE International Ultrasonics Symposium*. IEEE, 2014, pp. 305–308.

[11] S. Akhbari, F. Sammoura, C. Yang, M. Mahmoud, N. Aqab, and L. Lin, "Bimorph pmut with dual electrodes," in *IEEE 28th International Conference on Micro Electro Mechanical Systems (MEMS)*. IEEE, 2015, pp. 928–931.

[12] O. Rozen, S. T. Block, X. Mo, W. Bland, P. Hurst, J. M. Tsai, M. Daneman, R. Amirtharajah, and D. A. Horsley, "Monolithic mems-cmos ultrasonic rangefinder based on dual-electrode pmuts," in *IEEE 29th International Conference on Micro Electro Mechanical Systems (MEMS)*. IEEE, 2016, pp. 115–118.

[13] T. Wang and C. Lee, "Electrically switchable multi-frequency piezoelectric micromachined ultrasonic transducer (pmut)," in *IEEE 29th International Conference on Micro Electro Mechanical Systems (MEMS)*. IEEE, 2016, pp. 1106–1109.

[14] Y. Lu and D. A. Horsley, “Modeling, fabrication, and characterization of piezoelectric micromachined ultrasonic transducer arrays based on cavity soi wafers,” *Journal of Microelectromechanical Systems*, vol. 24, no. 4, pp. 1142–1149, 2015.

[15] C. Y. Wang and C. Wang, *Structural vibration: Exact solutions for strings, membranes, beams, and plates*. CRC Press, 2016.

[16] M. Kwak, “Vibration of circular plates in contact with water,” *Journal of Applied Mechanics*, vol. 58, no. 2, pp. 480–483, 1991.